Enhancing associative learning in rats with a computationally designed training protocol

Zhang, Xu O; Zhang, Yili; Engelke, Douglas S; Cho, Claire E; Smolen, Paul; Byrne, John H; Do-Monte, Fabricio H[#].

#Corresponding author:
Fabricio H. Do Monte, DVM, PhD.
Department of Neurobiology and Anatomy
McGovern Medical School
The University of Texas Health Science Center at Houston
Houston, Texas 77030
Phone: 713-500-5613
Email: fabricio.h.domonte@uth.tmc.edu

Keywords: Associative memory, fear conditioning, fear extinction, long-term potentiation, learning model, spaced learning.

ABSTRACT

Associative learning requires the activation of protein kinases with distinct temporal dynamics. Learning protocols with computationally designed intertrial intervals (ITIs) that maximize the interaction between fast-activated protein kinase A (PKA) and slow-activated extracellular signal-regulated kinase (ERK) enhance nonassociative learning in *Aplysia*. Here, we tested whether an optimal learning protocol with irregular ITIs, predicted computationally to increase the overlap between PKA and ERK signaling in rat hippocampus, would enhance associative learning in mammals. We simulated

~1000 training protocols with irregular ITIs and identified an optimal protocol, predicted to induce stronger associative learning than standard protocols with fixed ITIs. With auditory fear conditioning, we showed that male adult rats exposed to the optimal conditioning protocol exhibited stronger fear memory retrieval and impaired fear memory extinction, compared to rats that received either massed or spaced conditioning protocols with fixed ITIs. With fear extinction, we likewise observed that fear conditioned rats exposed to the optimal extinction protocol showed improved extinction of contextual fear memory, compared to rats that received standard extinction protocols. Together, these findings demonstrate the capacity of a behavioral intervention driven by a computational model of memory-related signaling pathways to enhance associative learning in mammals and may provide greater insight into strategies to improve cognition in humans.

INTRODUCTION

Long-term memory (LTM) formation that lasts for days to years is believed to be mediated by synaptic plasticity including long-term potentiation (LTP) or its invertebrate analogue long-term facilitation (LTF), which require gene expression and protein synthesis (Martin et al., 2000; Kandel, 2001; Lynch, 2004; Alberini, 2009; Byrne and Hawkins, 2015). Studies in the last decades have investigated LTP/LTF and their underlying molecular processes as potential targets to enhance learning or restore

memory deficits in laboratory animals. However, traditional interventions using systemic cognitive enhancers or intracerebral pharmacological manipulations (Sharif et al., 2021; Lauterborn et al., 2016; McGaugh and Petrinovich, 1965; Lynch et al., 2014; Fernandez et al., 2008) are either based on trial-and-error approaches in specific model systems or are highly invasive, making the translation of such interventions difficult for human applications. The recent development of neural recording and optogenetic techniques has enabled precise control of neurons based on their intrinsic firing rates in order to enhance learning or modify memories (Brown et al., 2012; Nabavi et al., 2014; Lee et al., 2017; Liu et al., 2012), but the use of these techniques in humans remains unforeseeable in the near future.

An alternative approach to enhance learning and memory is to develop computational models to predict optimal training protocols based on the intracellular molecular cascades that underlie LTM formation and LTP/LTF induction (Smolen et al., 2016; Smolen et al., 2020; Zhang et al., 2021). Previous studies have identified activation of PKA (Schacher et al., 1988; Goldsmith and Abrams, 1991; Muller and Carew, 1998) and of the mitogen-activated protein kinase (MAPK) isoform ERK (Martin et al., 1997; Sharma and Carew, 2004; Sharma et al., 2003) as essential cascades for LTF. These two pathways converge to phosphorylate transcriptional factors such as cAMP responsive element binding protein (CREB), which subsequently induce expression of multiple plasticity-related genes (Dash et al., 1990; Bartsch et al., 1995; Liu et al., 2011). The observation that that these two pathways exhibit distinct kinetics of activation (Muller and Carew, 1998; Philips et al., 2007; Zhang et al., 2021), suggests

72 that the temporal activity patterns, and activation overlap, of these pathways may
73 constitute an important target to enhance associative learning. Accordingly, our
74 previous study demonstrated that a computationally designed protocol with irregular ITIs
75 predicted to maximize the overlap of PKA and ERK activities enhances LTF and
76 nonassociative learning, specifically the long-term sensitization of the tail elicited
77 siphon-withdrawal reflex in *Aplysia* (Zhang et al., 2011).
78
79 Substantial similarities between molecular processes of LTF in invertebrates and LTP in
80 mammals make it plausible that the same strategies used to enhance LTF and
81 nonassociative learning in invertebrates could enhance LTP and associative learning in
82 mammals. PKA activation in rodent hippocampus and amygdala is required for LTP and
83 LTM (Schafe and LeDoux, 2000; Abel et al., 1997). Similarly, activation of ERK/MAPK
84 cascades and their cross-talk with PKA kinase are required for the phosphorylation of
85 CREB and LTP induction (Adams and Sweatt, 2002; Impey et al., 1998). Albeit with
86 different kinetics than observed in invertebrates, PKA and ERK activation in mammals
87 also differ considerably in temporal dynamics (Roberson and Sweatt, 1996; Vázquez et
88 al., 2000; Wang et al., 2014), providing a similar opportunity to maximize their overlap
89 with irregular ITIs in an attempt to enhance memory formation.
90
91 Here, we tested if the invertebrate LTF model (Zhang et al., 2011) can be adapted to
92 computationally design an optimal associative learning protocol in mammals. Empirical
93 data from the literature were used to model PKA and ERK dynamics in rat hippocampus
94 (Wang et al., 2014; Roberson and Sweatt, 1996; Vázquez et al., 2000), a critical brain

region implicated in the formation of associative memories in mammals (Milner et al., 1998; Mayes et al., 2007; Nakazawa et al., 2002). Then we simulated ~1000 different training protocols with irregular ITIs and identified an optimal protocol, predicted to induce stronger memory than standard training protocols with fixed ITIs. Using auditory fear conditioning and fear extinction paradigms in rats, we confirmed that our computationally designed protocol enhanced the acquisition as well as the extinction of fear memories in mammals. This strategy may have potential clinical relevance for interventions aiming at facilitating memory formation in psychiatric disorders associated with cognitive impairment in humans, as well as to enhance extinction-based therapies in patients suffering from fear-related disorders.

MATERIALS AND METHODS

Animals

All experimental procedures were approved by the Center for Laboratory Animal Medicine and Care of The University of Texas Health Science Center at Houston. National Institutes of Health guidelines for the care and use of laboratory animals were strictly followed in order to minimize any potential discomfort and suffering. A total of 120 male Long-Evans hooded adult rats (Charles Rivers Laboratories) 3-5 months of age and weighing 330-450 g were used. Rats were kept in a 12-hour light/12-hour dark cycle with food and water *ad libitum*. Experiments were conducted during the light phase. For the Optimal Extinction experiment, animals were maintained on a restricted diet of 18 g per day of standard laboratory rat chow to increase their motivation during

118 the lever press training. Rats' weights were monitored weekly to make sure that all
119 animals maintained their weight under food restriction.
120
121 **Model Development**
122 The mathematical model for the activation of kinase cascades critical for long-term
123 memory (LTM) was modified from a previous model of the signaling cascades for the
124 induction of long-term synaptic facilitation (Zhang et al., 2011). As mentioned above, the
125 induction of LTM for fear conditioning is known for requiring the activation of multiple
126 kinase cascades with different temporal dynamics. In the model, the cyclic AMP (cAMP)-
127 PKA pathway is rapidly activated after training, whereas the Raf- MEK-ERK pathway is
128 slowly activated, and both are required for the induction of LTM after fear conditioning
129 and extinction (**Fig. 1A, Fig. 4A**).
130 PKA Pathway. The dynamics of cAMP activation upstream of PKA following
131 training and the cAMP-dependent activation of PKA are described by Eqs. 1-4. Inactive
132 PKA is a holoenzyme (PKA_{RC}, Eq. 2), consisting of regulatory (PKA_R, Eq. 3) and catalytic
133 (PKA_C, Eq. 4) subunits. In response to training, represented by the variable *Stim* in Eq.
134 1, cAMP is activated (Eq. 1). Active cAMP binds to the regulatory subunit of PKA, leading
135 to the release of free, active catalytic subunit (Fig. 1A) (Eqs. 2-4). '*Stim*' represents the
136 neurotransmitters released by training that function to activate kinase cascades.
137
138 $$\frac{d[cAMP]}{dt} = \lambda \frac{[Stim]}{[Stim] + K_{Stim}} - k_{b,cAMP}[cAMP] \qquad \text{(Eq. 1)}$$
139 $$\frac{d[PKA_{RC}]}{dt} = k_{b,PKA}[PKA_C][PKA_R] - k_{f,PKA}[PKA_{RC}][cAMP]^2 \qquad \text{(Eq. 2)}$$

140 $$\frac{d[PKA_R]}{dt} = k_{f,PKA}[PKA_{RC}][cAMP]^2 - k_{b,PKA}[PKA_C][PKA_R] \quad \text{(Eq. 3)}$$

141 $$\frac{d[PKA_C]}{dt} = k_{f,PKA}[PKA_{RC}][cAMP]^2 - k_{b,PKA}[PKA_C][PKA_R] \quad \text{(Eq. 4)}$$

142 Parameter values are modified from Zhang et al. (2011) to activate PKA immediately
143 after training, but with PKA activity quickly returning to the basal in ~5 min (Fig. 1B)
144 (Roberson and Sweatt, 1996; Vázquez et al., 2000): λ = 14.6 μM/min, K_{STIM} = 85 μM,
145 $k_{b,cAMP}$ = 4 min^{-1}, $k_{f,PKA}$ = 20 μM^{-2}min^{-1}, $k_{b,PKA}$ = 12 μM^{-1}min^{-1}
146

147 ERK Pathway. The activation of ERK by training '*Stim*' is via sequential activation
148 of the upstream kinases Raf and MEK (Fig. 1A). Raf activates the MAP kinase kinase
149 MEK, MEK in turn activates the MAP kinase ERK. The differential equations describing
150 the activation of Raf, MEK, and ERK (Eqs. 5-12) are similar to those in Zhang et al. (2011).
151 However, a discrete time delay in activation of Raf was removed from the phosphorylation
152 of Raf (Eq. 5). Instead, based on empirical data (Wang et al., 2014; Ajay and Bhalla,
153 2004), parameters describing the activation of Raf were adjusted from Zhang et al. (2011)
154 so that the ERK activation curve reached the peak around 20 min post-training (Fig. 1B).

155 $$\frac{d[Raf^p]}{dt} = k_{f,Raf}[Raf][Stim] - k_{b,Raf}[Raf^p] \quad \text{(Eq. 5)}$$

156 $$[Raf] = [Raf]_{total} - [Raf^p] \quad \text{(Eq. 6)}$$

157 $$\frac{d[MEK]}{dt} = \frac{k_{b,MEK}[MEK^p]}{[MEK^p] + K_{MEK,2}} - \frac{k_{f,MEK}[Raf^p][MEK]}{[MEK] + K_{MEK,1}} \quad \text{(Eq. 7)}$$

158 $$\frac{d[MEK^{pp}]}{dt} = \frac{k_{f,MEK}[Raf^{p}][MEK^{p}]}{[MEK^{p}] + K_{MEK,1}} - \frac{k_{b,MEK}[MEK^{pp}]}{[MEK^{pp}] + K_{MEK,2}} \quad \text{(Eq. 8)}$$

159 $$[MEK^{p}] = [MEK]_{total} - [MEK] - [MEK^{pp}] \quad \text{(Eq. 9)}$$

160 $$\frac{d[ERK]}{dt} = \frac{k_{b,ERK}[ERK^{p}]}{[ERK^{p}] + K_{ERK,2}} - \frac{k_{f,ERK}[MEK^{pp}][ERK]}{[ERK] + K_{ERK,1}} \quad \text{(Eq. 10)}$$

161 $$\frac{d[ERK^{pp}]}{dt} = \frac{k_{f,ERK}[MEK^{pp}][ERK^{p}]}{[ERK^{p}] + K_{ERK,1}} - \frac{k_{b,ERK}[ERK^{pp}]}{[ERK^{pp}] + K_{ERK,2}} \quad \text{(Eq. 11)}$$

162 $$[ERK^{p}] = [ERK]_{total} - [ERK] - [ERK^{pp}] \quad \text{(Eq. 12)}$$

163 Parameter values: $k_{f,Raf}$ = 0.001 $\mu M^{-1} min^{-1}$, $k_{b,Raf}$ = 0.05 min^{-1}, $[Raf]_{total}$ = 0.5 μM,

164 $k_{f,MEK}$ = 0.41 min^{-1}, $k_{b,MEK}$ = 0.04 μM/min, $K_{MEK,1}$ = 0.20 μM,

165 $K_{MEK,2}$ = 0.19 μM, $[MEK]_{total}$ = 0.5 μM, $k_{f,ERK}$ = 0.41 min^{-1},

166 $k_{b,ERK}$ = 0.12 μM/min, $K_{ERK,1}$ = 0.19 μM,

167 $K_{ERK,2}$ = 0.21 μM, $[ERK]_{total}$ = 0.5 μM.

168 As in Zhang et al. (2011), a variable '*inducer*' was used to quantify the overlap of

169 activation between PKA and ERK, which together regulate the gene expression

170 necessary for the induction of LTM.

171 $$inducer = k_{inducer}\,[PKA_C]\,[ERK^{pp}] \quad \text{(Eq. 13)}$$

172 where $k_{inducer}$ = 1 μM^{-1}.

173 To determine which protocols could more effectively activate *inducer,* four-trial
174 protocols with three ITIs, each ranging from 2–20 min in steps of 2 min, were simulated.
175 Combining these permutations yielded 10^3 protocols. For each protocol, the maximal
176 (peak) overlap between PKA and ERK was quantified as the peak level of *inducer*
177 produced. Also, the value of *Stim* was varied from 100 to 300 μM to represent weak and
178 strong trainings and to test the robustness of protocols. Based on the maximal overlap,
179 a protocol with ITIs of 8, 8, and 16 min was selected and was denoted optimal partial
180 conditioning (OPC). We assumed that fear conditioning and extinction activate the same
181 signaling pathways, so we predicted this protocol would similarly enhance extinction.
182 Numerical methods. Fourth-order Runge-Kutta integration was used for
183 integration of all differential equations with a time step of 3 s. Further time step reduction
184 did not lead to significant improvement in accuracy. The steady-state levels of variables
185 were determined after at least one simulated day, prior to any manipulations. The model
186 was programmed in XPPAUT (http://www.math.pitt.edu/~bard/xpp/xpp.html) (Ermentrout,
187 2002) and simulated on Dell Precision T1700 microcomputers.
188
189
190 **Behavioral Tasks**
191 ***Optimal Conditioning***
192 *Apparatuses*
193 Two distinct chambers (context A and context B) positioned inside sound attenuating
194 boxes were used during the Optimal Conditioning experiments. Context A consisted of a
195 small operant chamber (34 cm high x 25 cm wide x 23 cm deep, 200 lux, Med

196 Associates, see schematic drawing in Fig. 2A top) with one of the two aluminum walls
197 covered by black adhesive paper and two transparent acrylic walls, and a metal grid
198 floor beneath which a microcentrifuge tube (Eppendorf) containing 50 µl of 10% amyl
199 acetate (Sigma-Aldrich) was positioned. Context B consisted of a larger acrylic operant
200 chamber (40 cm high x 50 cm wide x 26 cm deep, 20 lux, Med Associates, see
201 schematic drawing in Fig. 2A bottom) with one of its walls covered by a black and white
202 stripped paper, and a floor made of a white acrylic board beneath which a
203 microcentrifuge tube (Eppendorf) containing 50 µl of deionized water was positioned.
204
205 *Procedures*
206 On day 0, rats were placed in context A for a 20-min familiarization session. Next, rats
207 were assigned to three experimental groups by matching their baseline freezing and
208 locomotor activity during the familiarization session: Full Conditioning (FC), Partial
209 Conditioning (PC), and Optimal Partial Conditioning (OPC). On day 1, rats were placed
210 into context A and exposed to one nonreinforced habituation tone (3 kHz, 75 dB, 30 s)
211 followed by distinct fear conditioning protocols (44 min duration). The FC group received
212 eight presentations of a conditioned stimulus (CS, 3 kHz tone, 75 dB, 30 s) that co-
213 terminated with an unconditioned stimulus (US, footshock, 0.7 mA, 0.5 s), with fixed ITIs
214 of 270 s. The PC group received four similar CS-US pairings with the same ITIs of 270
215 s, and remained in the chamber until the end of the session. The OPC group received
216 four similar CS-US pairings with ITIs of 8, 8, and 16 min. On day 2, rats were placed in
217 context B and given two CS presentations (ITI of 150 s, 7 min duration) in the absence
218 of US to test the retrieval of tone-associated fear memory in a novel context. On day 3,

219 rats were returned to context A for an extinction training session where they received
220 twelve CS presentations (ITIs of 150 s, 37 min duration). The first four CSs were
221 compared to the last four CSs to assess extinction learning within the same session. On
222 day 4 and 5, rats were placed back in context A and B, respectively, and exposed to an
223 extinction retrieval session (similar to day 2). On day 29 and 30, rats were placed back
224 in context A and B, respectively, and exposed to a spontaneous recovery session
225 (similar to day 2). On day 1 and day 2, rats in the same group were trained
226 simultaneously in four chambers with the group order counterbalanced to avoid
227 interference from different protocols in neighboring chambers. On the following days,
228 rats were simultaneously tested in four chambers regardless of the group assignment.
229 Each rat was tested in the exact same chamber across the days. Footshocks, tones,
230 intertrial intervals, and session duration were controlled by an automated video tracking
231 system (ANY-maze, Stoelting), which also quantified the percentage of time freezing,
232 distance traveled, average speed and maximum speed. All rats passed the criteria of
233 20% of freezing during at least one CS of the fear conditioning session and the first two
234 CSs of the extinction session.
235
236 ***Optimal vs. Spaced Partial Conditioning***
237 *Apparatus and Procedures*
238 The same apparatus and contexts described above were used. Following familiarization
239 on Day 0, rats were randomly assigned to two groups: Optimal Partial Conditioning
240 (OPC) and Spaced Partial Conditioning (SPC). The same procedures described above
241 were used here, except that: *i)* the footshock intensity was reduced from 0.7 mA to 0.5

242 mA to decrease the possibility of ceiling effects; *ii)* the SPC group received four CS-US
243 pairings with ITIs of 11 min and 10 s. The same automated video tracking system (ANY-
244 maze, Stoelting) described above was used for protocol control and behavioral
245 quantification. One rat that failed the criteria of 20% of freezing during at least one CS of
246 the fear conditioning session and the first two CSs of the extinction session was
247 excluded from the analyses.
248
249 ***Optimal Extinction***
250 *Lever-press training*
251 Rats were placed in an acrylic/aluminum operant chamber (34 cm high x 25 cm wide x
252 23 cm deep, Med Associates, see schematic drawing in Fig. 4A) and trained to press a
253 lever for sucrose on a fixed ratio of one pellet for each press. Next, animals were trained
254 in a variable interval schedule of reinforcement that was gradually reduced across the
255 days (one pellet every 15 s, 30 s, or 60 s) until they reached a minimum criterion of 10
256 presses/min after 7 days of training. All sessions lasted 30 min and were performed on
257 consecutive days. Sucrose pellet delivery, variable intervals, and session duration were
258 controlled by an automated video tracking system (ANY-maze, Stoelting).
259
260 *Apparatus and Procedure*
261 On day 8, rats were placed into the same chamber where they had previously
262 undergone lever presses training. Animals were exposed to five nonreinforced
263 habituation tones (3 kHZ, 75 dB, 30 s duration) followed by seven CS-US pairings (ITIs
264 of 150 s, 37 min duration). The footshock intensity was increased from 0.7 mA to 1.0-

265 1.2 mA to result in stronger fear acquisition and consequently higher freezing levels
266 during the extinction training session in the next day. Rats were assigned to three
267 experimental groups by matching their freezing and lever presses during the fear
268 conditioning session: Full Extinction (FE), Partial Extinction (PE), and Optimized Partial
269 Extinction (OPE). On day 9, rats were returned to the same chamber for a fear
270 extinction session (39 min duration). The FE group received twelve CSs with ITIs of 150
271 s; the PE group received four CSs with ITIs of 150 s and remained in the chamber until
272 the end of the session; and the OPE group received four CSs with ITIs of 8, 8, and 16
273 min. On day 10 and 35, rats were placed into the same chamber and received two CSs
274 with an ITI of 150 s to test the strength of fear extinction memory during extinction
275 retrieval and spontaneous recovery tests, respectively. The same automated video
276 tracking system (ANY-maze, Stoelting) described above was used for protocol control
277 and behavioral quantification. Two rats that never reached the criterium of 20% of
278 freezing during at least one CS of the fear conditioning session and the first two CSs of
279 the extinction session were excluded from the analyses.
280
281 **Quantification and statistical analysis**
282 Rats were recorded with digital video cameras (Logitech C920) and behavioral indices
283 were measured using automated video-tracking system (ANY-maze). Lever presses per
284 minute were calculated by measuring the number of presses during the 30 s cue (or 30
285 s pre-cue) multiplied by two. All graphics and numerical values reported in the figures
286 are presented as mean ± standard error of the mean (SEM). Grubbs's tests were used
287 to identify outliers ($p < 0.05$) in each experiment and one rat in Fig. 2 was removed after

identified by the test. Shapiro-wilk test was performed to determine whether the data have a normal distribution. F test before pair-wise comparison and Brown-Forsythe test before multiple group comparison were performed to test if groups have the same variance. Statistical significance for parametric distributions was determined with paired Student's t test, Welch's t test, one-way analysis of variance (ANOVA) or two-way repeated-measures ANOVA followed by Tukey post-hoc comparisons, whereas Kruskal-Wallis test followed by Dunn's post-hoc test was used for non-parametric distributions (Prism 7), as indicated for each experiment. Sample size was based on estimations from previous literature and experience.

Data availability

All data that support the findings presented in this study are available from the corresponding author on reasonable request. Source codes will be submitted to the ModelDB database (McDougal et al., 2015), and to GitHub (link to be updated).

RESULTS

A computational model based on PKA and ERK dynamics in rats identified an optimal partial fear conditioning protocol

Our model previously used in *Aplysia* (Zhang et al., 2011) was adapted to simulate the dynamics of PKA and ERK during the process of LTP induction in rat hippocampus (**Fig. 1A**). In this model, the stimulus (*Stim*), which represents tetanic stimuli, rapidly activates PKA via the cAMP pathway and slowly activates ERK via the Raf-MEK

311 pathway. The synergistic interaction between PKA and ERK pathways is quantified by a
312 variable *inducer*, which corresponds to the efficacy of the stimulus in inducing LTP. ERK
313 kinetics were described by differential equations (see Methods) with parameter values
314 reproducing empirical findings that ERK activity reaches peak levels 15~20 min after
315 BDNF treatment or tetanic stimuli in rat hippocampus acute slices (Wang et al., 2014;
316 Ajay and Bhalla, 2004). Equations describing PKA kinetics simulated data showing that
317 PKA is transiently activated within 2 min after LTP induction in slices from rat
318 hippocampus or within 5 min *in vivo* after spatial discrimination task training (Roberson
319 and Sweatt, 1996; Vázquez et al., 2000). We used this model to simulation fear
320 conditioning in rats, in which the pairing of a conditioned stimulus (CS) with an
321 unconditioned stimulus (US) is represented by *Stim*, and the conditioned responses are
322 proportional to the peak value of *inducer*. We observed that a single CS-US pairing
323 produced little overlap between PKA and ERK pathways (**Fig. 1B1**). We then simulated
324 ~1000 partial fear conditioning protocols, with 4 trials and varying ITIs, to identify one
325 predicted to have optimal ITIs for triggering downstream gene activation. To compare,
326 we also simulated a Full Conditioning (FC) protocol with 8 trials and a fixed ITI of 270 s,
327 and a Partial Conditioning (PC) protocol with 4 trials and the same ITI of 270 s, which
328 resemble previous protocols used for full and partial fear conditioning in rats (Detert et
329 al., 2008; Lonsdorf et al., 2017). Our simulation identified an Optimal Partial
330 Conditioning (OPC) protocol with 4 trials and irregular ITIs of 8, 8, and 16 min, which
331 was able to produce higher peak *inducer* than the standard PC protocol (**Fig. 1B2-1B4**).
332 Based on our simulation, we predicted that the computationally designed OPC protocol
333 would produce stronger long-term memory in rats than the standard PC protocol.

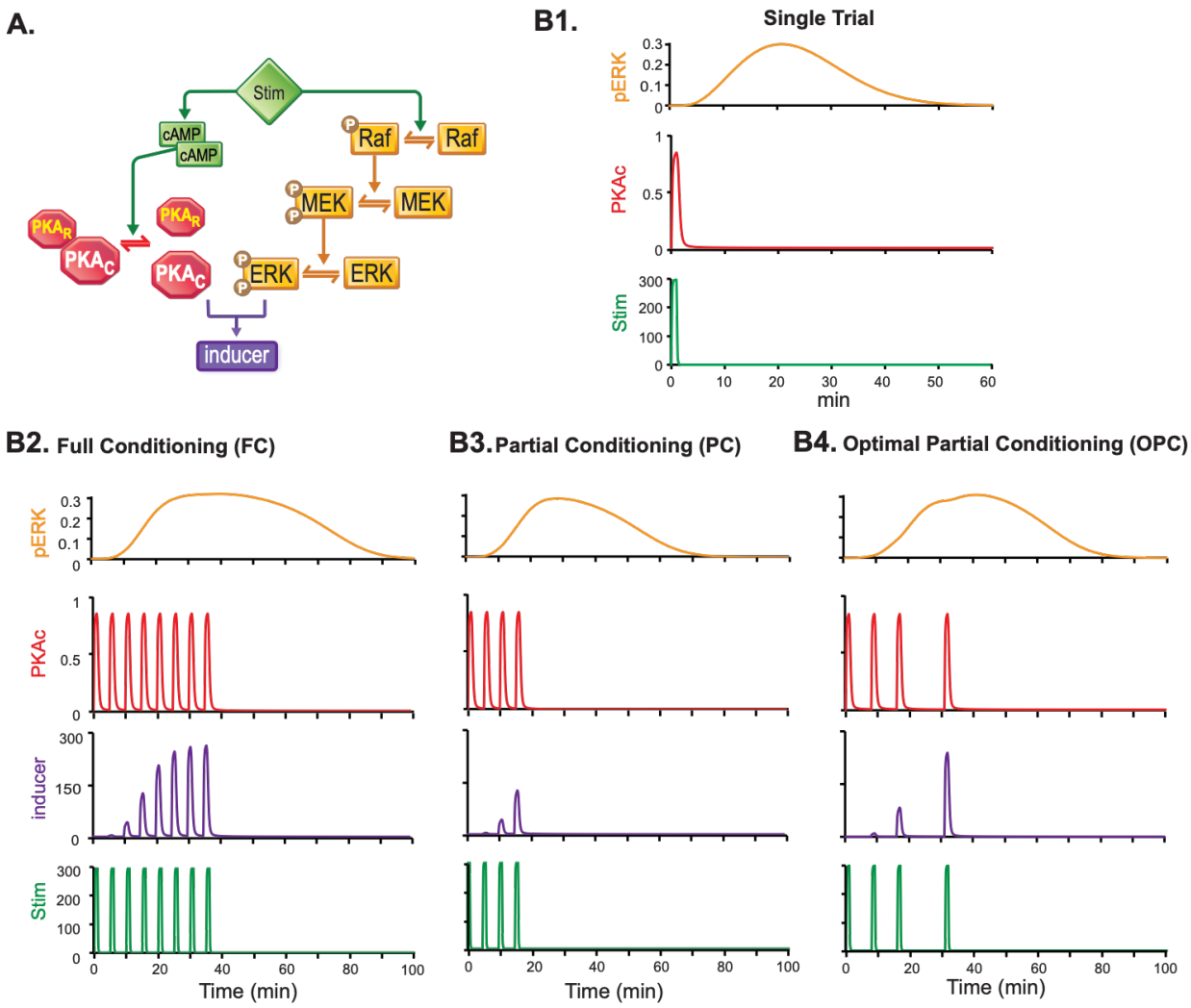

Figure 1. Computational simulations of PKA and ERK pathways predict an optimal protocol for fear conditioning. A, Schematic of the model. Stimulus (*Stim*) activates PKA via cAMP and activates ERK via Raf-MEK. The variable *inducer* quantifies the PKA/ERK interaction (activity overlap). **B1**, Simulated time courses of activated ERK (pERK, orange traces, μM) and activated PKA (PKAc, red traces) in response to one trial of *Stim* (μM). **B2**, Simulated time courses of pERK (orange traces, μM), PKAc (red traces) and *inducer* (violet traces, nM) in response to an 8-trial protocol with regular ITIs of 4.5 min (full conditioning, FC). **B3**, Simulated time courses of pERK (orange traces), PKAc (red traces), and *inducer* (violet traces) in response to a 4-trial protocol with regular ITIs of 4.5 min (partial conditioning, PC). **B4**, Simulated time courses of pERK (orange traces), PKAc (red traces) and *inducer* (violet traces)

344 in response to a 4-trial protocol with computationally designed intervals (optimal partial conditioning,
345 OPC).
346
347 ***The optimal partial conditioning protocol induces stronger fear memory than a***
348 ***standard partial conditioning protocol***
349
350 To test if the computationally designed OPC protocol could enhance associative
351 learning in rats, we used a classical auditory fear conditioning paradigm. Because the
352 hippocampus is required for context encoding during fear conditioning (Phillips and
353 LeDoux, 1992; Selden et al., 1991; Maren et al., 2013), we used two different chambers
354 (context A and context B) to assess the contribution of the context to the auditory fear
355 memory. The two contexts differed in size, floor texture, visual decoration of the walls,
356 and odor cues (**Fig. 2A**). On Day 0, rats were pre-exposed to context A for 20 min to
357 familiarize with the chamber where fear conditioning took place in the following day.
358 After matching their baseline freezing and locomotor activity during the familiarization
359 session (**Fig. S1**), rats were assigned to one of the three experimental groups described
360 above in our simulation experiments: Full Conditioning (FC), Partial Conditioning (PC),
361 and Optimal Partial Conditioning (OPC). On Day 1, rats were placed into context A and
362 exposed to one nonreinforced habituation tone (3 kHZ, 75 dB, 30 s) followed by distinct
363 fear conditioning protocols (44 min duration, **Fig. 2B**). The FC group received eight
364 presentations of CS (3 kHZ tone, 75 dB, 30 s) that co-terminated with an US (footshock,
365 0.7 mA, 0.5 s) with ITIs of 270 s. The PC group received four similar CS-US pairings
366 with the same ITIs of 270 s, and remained in the chamber until the end of the session to
367 equate the total context exposure time. The OPC group received four similar CS-US

368 pairings with ITIs of 8, 8, and 16 min. All groups reached high levels of freezing (> 65%,
369 **Fig. 2C**) and reduced locomotion at the end of the fear acquisition session. On Day 2,
370 rats were placed in context B and given two CS presentations (ITI of 150 s, 7 min
371 duration) in the absence of US to test the retrieval of tone-associated fear memory in a
372 novel context. Compared to the FC group, both PC and OPC groups exhibited less
373 freezing during the second CS presentation (Two-way repeated measures (RM)
374 ANOVA followed by Tukey's post-hoc test. $F_{(2, 37)} = 3.751$, $P = 0.033$; FC vs. OPC: p =
375 0.029; FC vs. PC: p = 0.002; OPC vs. PC: p = 0.527). Nevertheless, both FC and OPC
376 groups showed reduced average speed during the retrieval test compared to the
377 standard PC group, suggesting stronger fear retrieval in a novel context (**Fig. 2D;** One-
378 way ANOVA followed by Tukey's post hoc test. $F_{(2, 37)} = 10.87$, $P < 0.001$; FC vs. OPC:
379 p = 0.131; FC vs. PC: p < 0.001; OPC vs. PC: p = 0.024). On Day 3, rats were returned
380 to context A for an extinction training session where they received twelve CS
381 presentations (ITIs of 150 s, 37 min duration). Although no significant differences in
382 freezing levels were observed among the groups during each CS presentation (Two-
383 way RM ANOVA. $F_{(22, 407)} = 1.169$, $P = 0.271$), a within session extinction analysis
384 comparing the first four CSs to the last four CSs revealed impaired extinction learning in
385 the FC and OPC groups, when compared to the PC group. This impairment in the
386 acquisition of extinction in the FC and OPC groups was characterized by sustained
387 freezing levels across the session, which differed from the PC group that showed
388 reduced freezing levels from the first to the last CSs presentation (**Fig. 2E left;** Paired
389 Student's t test. FC: $t_{13} = 2.153$, p = 0.051; PC: $t_{11} = 4.191$, p = 0.001; OPC: $t_{13} = 0.869$,
390 p = 0.400**)**. Interestingly, the OPC group exhibited persistent freezing levels during the

391 extinction training session as indicated by a reduced relative change in freezing from
392 the beginning to the end of the session, when compared to the PC group (**Fig. 2E right;**
393 One-way ANOVA followed by Tukey's post-hoc test. $F_{(2, 37)} = 3.315$, $P = 0.047$; FC vs.
394 OPC: p = 0.487; FC vs. PC: p = 0.320; OPC vs. PC: p = 0.037). Despite the persistent
395 freezing levels across the extinction training session observed in the OPC group, no
396 significant differences were found between the OPC and the PC groups during either
397 the extinction retrieval tests performed on Days 4 and 5 (Two-way RM ANOVA. context
398 A: $F_{(2, 37)} = 0.097$, $P = 0.907$; context B: $F_{(2, 37)} = 2.984$, $P = 0.063$) or the spontaneous
399 recovery tests performed on Days 29 and 30 (**Fig. 2C;** Two-way RM ANOVA followed
400 by Tukey's post hoc test. context A: $F_{(2, 37)} = 3.259$, $P = 0.049$; FC vs. OPC: p = 0.027;
401 FC vs. PC: p = 0.038; OPC vs. PC: p = 0.999; context B: $F_{(2, 37)} = 0.774$, $P = 0.469$).
402 Taken together, these data demonstrate that the computationally designed training
403 protocol (OPC) is able to enhance fear acquisition in rats, thereby resulting in a stronger
404 fear memory that is more resistant to extinction.

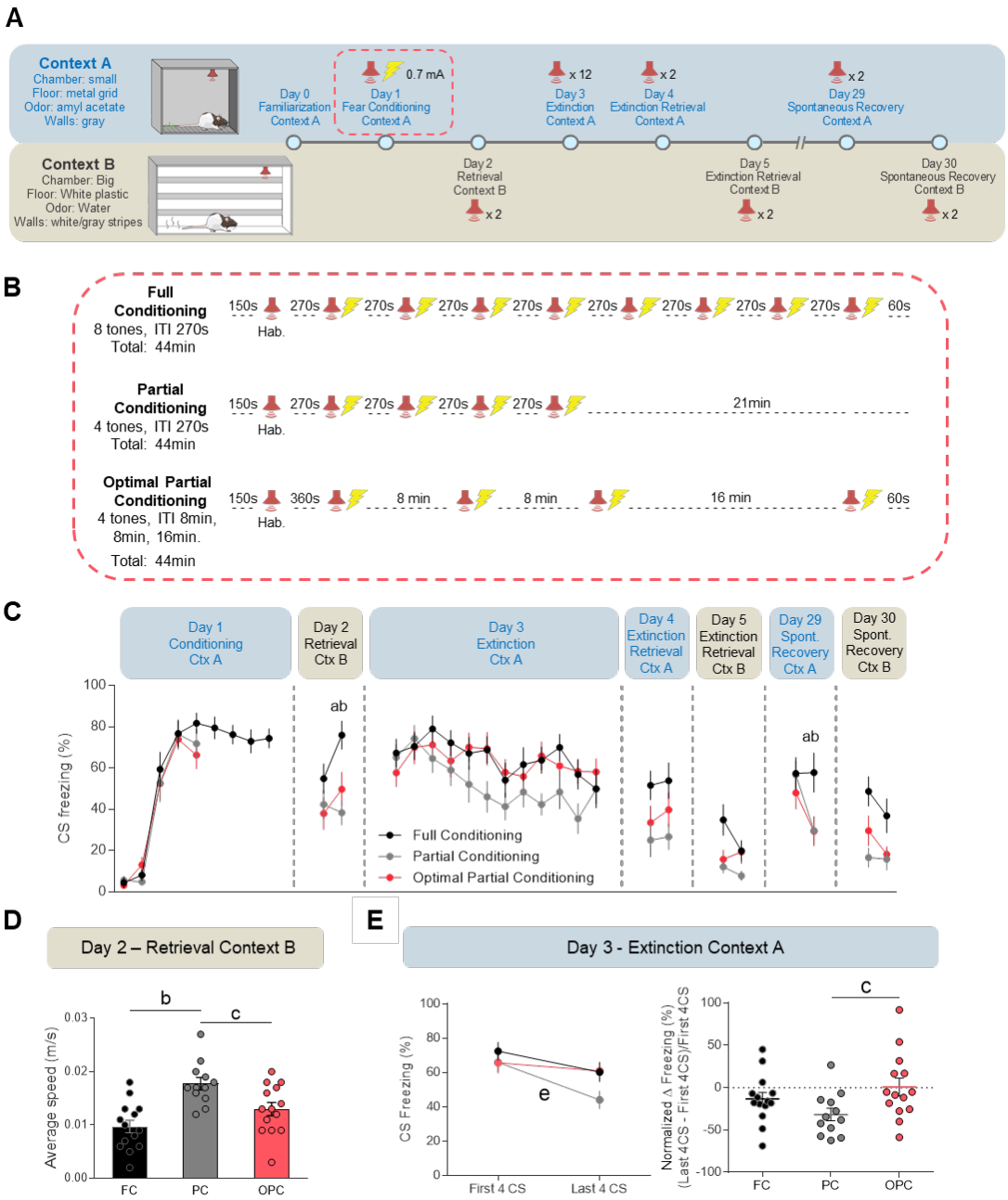

Figure 2. Computationally designed protocol enhanced fear conditioning in rats. **A,** Schematics of the enhanced fear conditioning experimental procedures. Top: tests that were conducted in Context A. Bottom: tests that were conducted in Context B. **B,** Schematics of the fear conditioning protocols for full conditioning (FC, n = 14), partial conditioning (PC, n = 12), and optimal partial conditioning groups (OPC, n = 14). Following a habituation (Hab.) tone, rats received multiple trials of a conditioned stimulus (CS, 3 kHz tone, 30 s) that co-terminated with an unconditioned stimulus (US, footshock, 0.7 mA, 0.5 s). **C,**

412 Freezing levels during CS presentations of each group across the experiment. Two-way Repeated-
413 Measure ANOVA for each day followed by Tukey's post hoc test. Letters a, b, and c indicate pairwise
414 post hoc tests with $p < 0.05$: a, FC vs. OPC; b, FC vs. PC; c, OPC vs. PC. **D,** OPC group shows lower
415 average speed compared to PC group. One-way ANOVA followed by Tukey post hoc test. Letters b and c
416 indicate pairwise tests with $p < 0.05$: b, FC vs. PC ; c, OPC vs. PC. **E,** OPC group is resistant to extinction
417 while PC group shows significantly more extinction. Left, the freezing levels during the first 4 and last 4
418 CS presentations. Paired Student's t test. Letter e indicates test with $p < 0.05$: PC, Last 4 CS vs. First 4
419 CS. Right, normalized change of the freezing level during extinction, as indicated by the difference of the
420 freezing levels between last 4 and first 4 CS presentations as a percentage of the freezing level of the
421 first 4 CS presentations. One-way ANOVA followed by Tukey's post hoc test. * $p<0.05$. Letter c indicates
422 pairwise test with $p < 0.05$: OPC vs. PC. Data shown here and in subsequent illustrations as mean ±
423 SEM.
424
425 ***The optimal partial conditioning protocol induces stronger fear memory than a***
426 ***spaced partial conditioning protocol***
427
428 Previous studies have demonstrated that spaced learning protocols result in stronger
429 memories than standard (i.e., massed) learning protocols in both humans (Cepeda et
430 al., 2006; Raman et al., 2010) and rodents (Anderson et al., 2008; Jiang et al., 2019;
431 Scharf et al., 2002; but also see Cain et al., 2003). Thus, an alternative explanation for
432 the augmented fear memory observed in the OPC group in Fig. 2 could be simply a
433 trial-spacing effect, because our standard PC group used massed CS-US pairings.
434 Indeed, there was a broad range of effective 4-trial protocols (**Fig. S2**), with one
435 protocol with fixed 11 min 10 s ITIs producing a nearly identical peak level of inducer as
436 the OPC protocol, and a higher peak level of inducer than other protocols with fixed ITIs

437 from 1 min to 21 min (**Fig. 3A1, Fig. S2A**). We termed this protocol the spaced partial
438 conditioning (SPC) protocol. We also examined the effects of different stimulus
439 intensities on predicting optimal training trials. The 1,000 different protocols were re-
440 simulated with a reduced intensity of stimulus. Interestingly, the protocol with 4 trials
441 and irregular ITIs of 8, 8, and 16 min still produced the greatest peak level of inducer
442 (**Fig. 3A2, Fig. S2B**). Equally interesting was that with weaker stimuli, the OPC protocol
443 became relatively more effective than the SPC protocol. Therefore, we predicted that
444 empirically, the irregular intervals of the OPC may produce more effective conditioning
445 than the SPC protocol. To test this hypothesis, we conducted an experiment to compare
446 the OPC and SPC protocols using a reduced shock intensity (0.5 mA instead of the 0.7
447 mA used in Fig. 2) (**Fig. 3B**). Rats were assigned to OPC or SPC groups by matching
448 their baseline freezing and locomotor activity during the familiarization session
449 (**Supplementary Fig. 1B**). During the fear acquisition, the SPC group received 4 CS-
450 US pairings with ITIs of 11 min and 10 s, whereas the OPC group was exposed to the
451 same protocol as in Fig. 2 (*i.e.*, 4 CS-US pairings with ITIs of 8, 8, and 16 min) (**Fig.
452 3C**). We found that the difference in the ITIs between the OPC and SPC groups was
453 sufficient to result in distinct levels of fear memory acquisition. Rats exposed to OPC
454 showed higher CS freezing levels during the third CS-US pairing of the fear acquisition
455 session (**Fig. 3D Day 1;** Two-way RM ANOVA followed by Tukey's planned
456 comparison. $F_{(4, 64)} = 1.550$, $P = 0.339$; OPC vs. SPC: p = 0.019). In addition, fear
457 memory retrieval was increased when rats in the OPC group were returned to context A
458 for an extinction training session on Day 3, as indicated by higher freezing during the
459 first two CS presentations, compared to the SPC group (**Fig. 3D Inset;** Welch's t test.

460 $t_{12.43}$ = 2.227, p = 0.045). Both OPC and SPC groups exhibited the same levels of
461 freezing by the end of the extinction training session (**Fig. 3D Day 3;** Two-way RM
462 ANOVA followed by Tukey's post hoc test. $F_{(11, 176)}$ = 2.997, P = 0.001; Tone 12, OPC
463 vs. SPC: p > 0.999), as well as during the extinction retrieval tests performed in context
464 A (**Fig. 3D Day 4;** Two-way RM ANOVA. $F_{(2, 37)}$ = 0.097, P = 0.907) or context B (**Fig.**
465 **3D Day 5;** Two-way RM ANOVA. $F_{(2, 37)}$ = 2.984, P = 0.629). However, fear memory
466 spontaneously recovered when rats in the OPC group were retested in context A
467 approximately 3 weeks later, as indicated by higher freezing during the first CS
468 presentation compared to SPC-trained rats (**Fig. 3D Day 29;** Two-way RM ANOVA
469 followed by Tukey's planned comparison. $F_{(2, 32)}$ = 1.809, P = 0.180; OPC vs. SPC: p =
470 0.030). In summary, these data suggest that the enhancement in fear memory
471 acquisition observed with our computationally designed OPC protocol cannot simply be
472 attributed to a trial-spacing effect or differences in the delay to remove the animals from
473 the chamber, but it is rather associated with the maximized overlap between PKA and
474 ERK signaling.

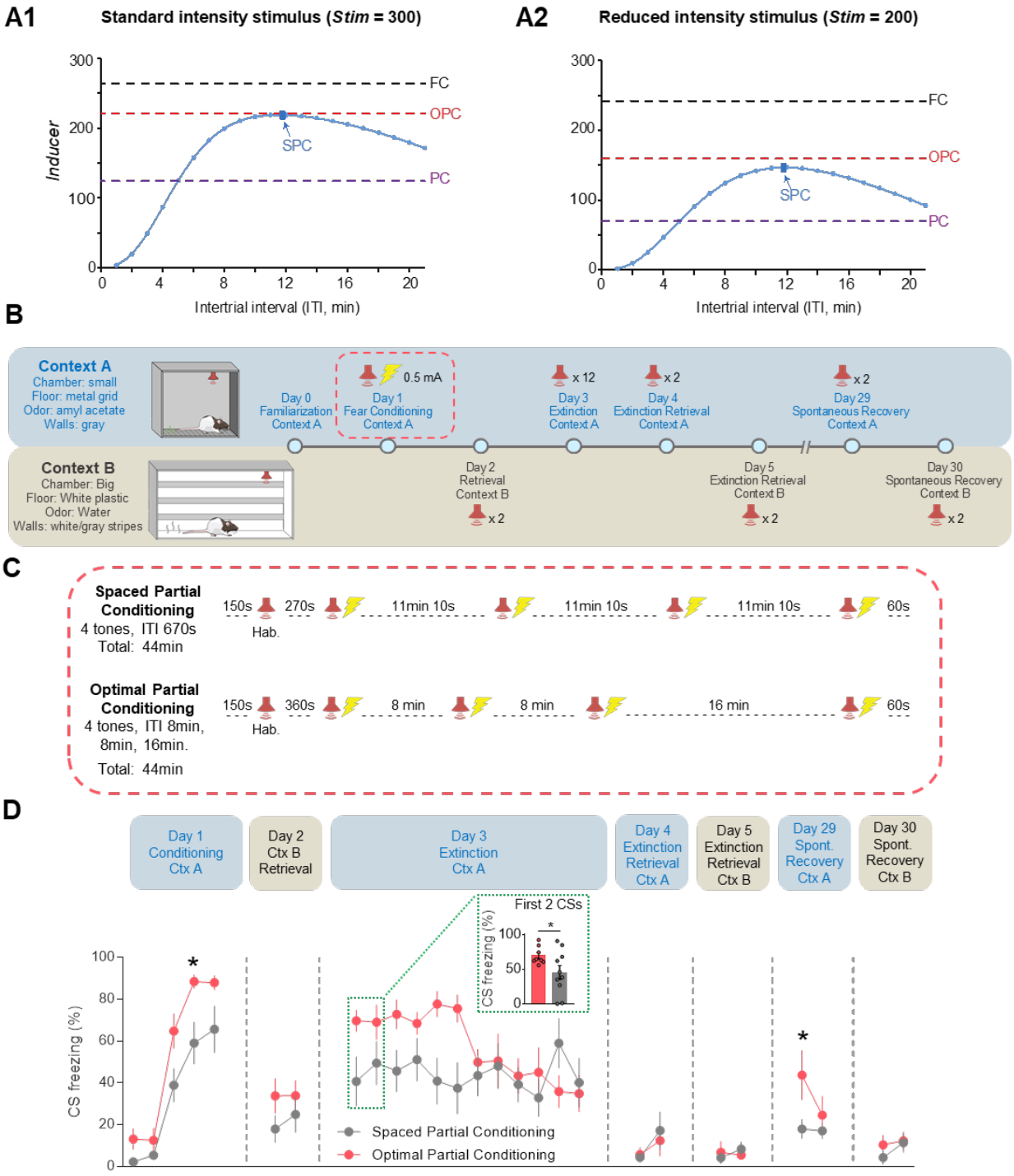

Figure 3. **Optimal partial conditioning protocol induced stronger fear memory than spaced partial conditioning protocol in rats**. **A**, *Inducer* peak levels from the FC, PC, and OPC protocols, compared to peak levels from partial conditioning protocols of 4 trials with regular ITIs varying from 1 to 21 min, using standard intensity stimulus (**A1**) or reduced intensity stimulus (**A2**). The peak *inducer* values of FC, PC,

480 and OPC are labeled by dashed lines (black: FC; red: OPC; purple: PC). The blue curve gives peak
481 *inducer* values for the protocols with regular ITIs, and the curve peaks at the dark blue dot and arrow,
482 representing the SPC protocol with equal ITIs of 11 min and 10 s. **B,** Schematics of the fear conditioning
483 procedures. Top: tests that were conducted in Context A. Bottom: tests that were conducted in Context B.
484 **C,** Schematics of the fear conditioning protocols for optimal partial conditioning (OPC, n = 8), and spaced
485 partial conditioning groups (SPC, n = 10, ITI = 670 s). Following a habituation (Hab.) tone, rats received 4
486 trials of a conditioned stimulus (CS, 3 kHz tone, 30 s) that co-terminated with an unconditioned stimulus
487 (US, footshock, 0.5 mA, 0.5 s). **D,** Freezing levels during CS presentations of each group across the
488 experiment; Two-way repeated-measure ANOVA for each day followed by Tukey's pairwise post hoc test,
489 * $p<0.05$. Inset: the average freezing level during the first two CS presentations; Welch's t test, * $p<0.05$.
490

491 ***The computationally designed optimal partial conditioning protocol also***
492 ***enhanced fear extinction***

493

494 Extinction is a new learning that temporarily inhibits the initial associative memory (de
495 Oliveira Alvares and Do-Monte, 2021; Quirk and Mueller, 2008). Because previous
496 studies suggest that the molecular mechanisms underlying fear extinction learning are
497 similar to those underlying fear acquisition (Berman and Dudai, 2001; Flood et al., 1977;
498 Radulovic and Tronson, 2010; Santini et al., 2001; Szapiro et al., 2003; Tronson et al.,
499 2008), we hypothesized that the computationally designed protocol would also enhance
500 the acquisition of extinction, suppressing the original fear memory. We therefore used
501 the OPC protocol with 4 trials and irregular ITIs of 8, 8, and 16 min as an Optimal Partial
502 Extinction (OPE) protocol (**Fig. 4B4**). We compared the OPE protocol with a Full
503 Extinction (FE, **Fig. 4B2**) protocol using 12 trials and ITIs of 150 s, and a Partial
504 Extinction (PE, **Fig. 4B3**) protocol using 4 trials and the same ITIs of 150 s, which

505 resemble previous protocols used for full and partial fear extinction in rats (Santini et al.,
506 2004; Holmes and Quirk, 2010; Do-Monte et al., 2015). Similar to the simulation results
507 for the conditioning protocols, the OPE protocol triggered higher peak *inducer* than the
508 PE protocol with equal ITIs of 150 s, and was comparable to the FE protocol (**Fig. 4B**).
509 We thus predicted the OPE protocol would result in stronger extinction of fear memory
510 than the standard PE protocol.

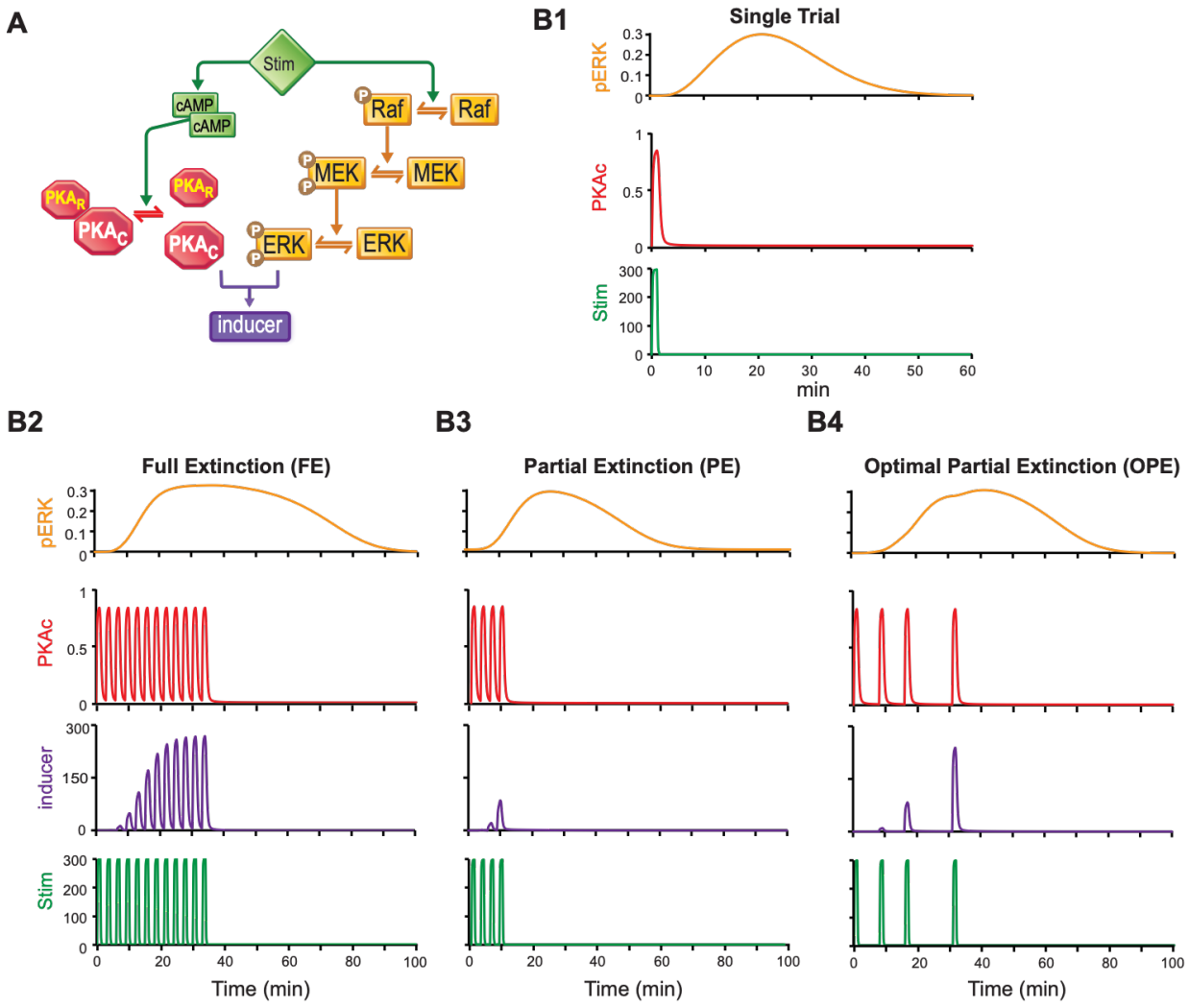

512 **Figure 4. Prediction of enhanced protocol for fear extinction. A**, Schematic of the model. **B1**,
513 Simulated time courses of activated ERK (pERK, orange traces, μM) and activated PKA (PKAc, red
514 traces) in response to one trial of *Stim* (μM). **B2**, Simulated time courses of pERK (orange traces, μM),

515 PKAc (red traces) and *inducer* (violet traces, nM) in response to 12-trial protocol with regular intervals of
516 2.5 min (full extinction, FE). **B3**, Simulated time courses of pERK (orange traces), PKAc (red traces) and
517 *inducer* (violet traces) in response to 4-trial protocol with regular intervals of 2.5 min (partial extinction,
518 PE). **B4**, Simulated time courses of pERK (orange traces), PKAc (red traces) and *inducer* (violet traces) in
519 response to 4-trial protocol with computationally designed intervals (optimal partial extinction, OPE).
520

521 To test this prediction, we designed an experiment comparing the efficacy of different
522 extinction protocols (**Fig. 5A**). We used conditioned suppression of reward-seeking
523 behavior as an additional measure of fear memory because lever-press suppression is
524 more sensitive than freezing during fear extinction paradigms (Mast et al., 1982; Sotres-
525 Bayon et al., 2012). In addition, lever presses help to maintain a constant level of
526 activity so that freezing can be more reliably measured along the session (Quirk et al.,
527 2000). Since lever presses for reward are trained in a specific context, and extinction
528 memory is context-dependent (Podlesnik et al., 2017; Goode and Maren, 2014), we
529 used only one context in this experiment so that lever press suppression can be
530 consistently assessed across sessions and the extinction memory can be retrieved after
531 the extinction learning. Rats were initially trained to press a lever to receive sucrose
532 pellets in a variable interval schedule of 60 s. After 7 days of training, rats reached the
533 same levels of lever pressing (~10 presses/min) and locomotor activity (**Supplementary**
534 **Fig. 1C**). On Day 8, they underwent a fear conditioning session which included five
535 nonreinforced habituation tones (3 kHZ, 75 dB, 30 s duration) followed by seven CS-US
536 pairings (ITIs of 150 s, 37 min duration). In simulations, the OPE group showed peak
537 levels of *inducer* comparable to the FE group and higher than the PE group when strong
538 stimuli were used. We therefore increased the footshock intensity from 0.7 mA to 1.0

539 mA, which resulted in stronger fear acquisition and consequently higher freezing levels
540 during the extinction session. This stimulus intensity also helped to avoid a “floor effect”
541 in the following tests. On Day 9, rats were assigned to three experimental groups by
542 matching their freezing and lever presses during the fear conditioning session: Full
543 Extinction (FE), Partial Extinction (PE), and Optimal Partial Extinction (OPE) (One-way
544 ANOVA. $F_{(14, 231)} = 0.404$, $P = 0.973$). On Day 10, rats were returned to the same
545 chamber for a fear extinction session (39 min duration). The FE group received twelve
546 CSs with ITIs of 150 s; the PE group received four CSs with ITIs of 150 s and remained
547 in the chamber until the end of the session; and the OPE group received four CSs with
548 ITIs of 8, 8, and 16 min (**Fig. 5B**). Our results revealed that at the end of the CS
549 presentations, freezing levels reduced from ~50% to ~20% in the FE groups, whereas
550 the PE and OPE groups maintained the same levels of freezing throughout the four CSs
551 (**Fig. 5C, Day 8**). Similarly, the FE group showed a significant increase in lever presses
552 (from 0.1 to 1.5 press/min) during the CS presentations from the beginning to the end of
553 the session, whereas CS lever presses remained unaltered in the PE and OPE groups
554 (**Supplementary Fig. 3A&B**; Paired Student’s t test; FE: $t_{11} = 2.837$, $p = 0.016$; PE: t_{10}
555 $= 1.000$, $p = 0.341$; OPE: $t_{12} = 1.237$, $p = 0.239$). However, the OPE group showed a
556 significant increase in lever presses during the 30-s periods that preceded the CS
557 presentations (pre-CS) when comparing the first two pre-CS periods to the last pre-CS
558 period of the extinction training session (**Fig. 5D&E**; Paired Student’s t test; FE: t_{11} =
559 0.994, $p = 0.341$; PE: $t_{10} = 1.111$, $p = 0.293$; OPE: $t_{12} = 3.773$, $p = 0.003$), suggesting
560 enhanced within-session extinction of contextual fear memory (Morgan and LeDoux,
561 1995). On Days 10 and 35, rats were returned to the same chamber and received two

562 CSs with an ITI of 150 s to test the strength of fear extinction memory during extinction
563 retrieval and spontaneous recovery tests, respectively. No significant difference in CS
564 freezing or CS lever presses were observed among the three groups during these tests
565 (**Fig. 5C, Day 10&35;** Two-way RM ANOVA. Day 10: Freezing, $F_{(2, 33)} = 0.207$, $P =$
566 0.814; Lever Presses, $F_{(2, 33)} = 0.069$, $P = 0.933$; Day 35: Freezing, $F_{(2, 33)} = 0.535$, $P =$
567 0.591; Lever Presses, $F_{(2, 33)} = 1.085$, $P = 0.350$). However, the OPE group showed
568 increased pre-CS lever pressing rate either in the first pre-CS period (**Fig. 5D;** Two-way
569 RM ANOVA followed by Tukey's planned comparison. $F_{(2, 33)} = 2.897$, $P = 0.069$; Tone
570 1, a, FE vs. PE, p = 0.791; b, FE vs. OPE, p = 0.025; c, OPE vs. PE, p = 0.005) or
571 when averaging the two pre-CS periods during the spontaneous recovery test (**Fig. 5F**;
572 Kruskal-Wallis's test followed by Dunn's post hoc test. $H(2) = 6.414$, $P = 0.041$; a: FE
573 vs. OPE, p = 0.531; b: FE vs. PE, p = 0.709; c: OPE vs. PE, p = 0.035), when compared
574 to the FE and PE groups on day 35. These results suggest that, although the tone-
575 associated memory was similar among the groups, our computationally designed OPE
576 protocol was able to enhance the extinction of contextual fear memory, as indicated by
577 enhanced within-session extinction of conditioned suppression and by reduced
578 conditioned suppression approximately 3 weeks after the extinction training session.
579

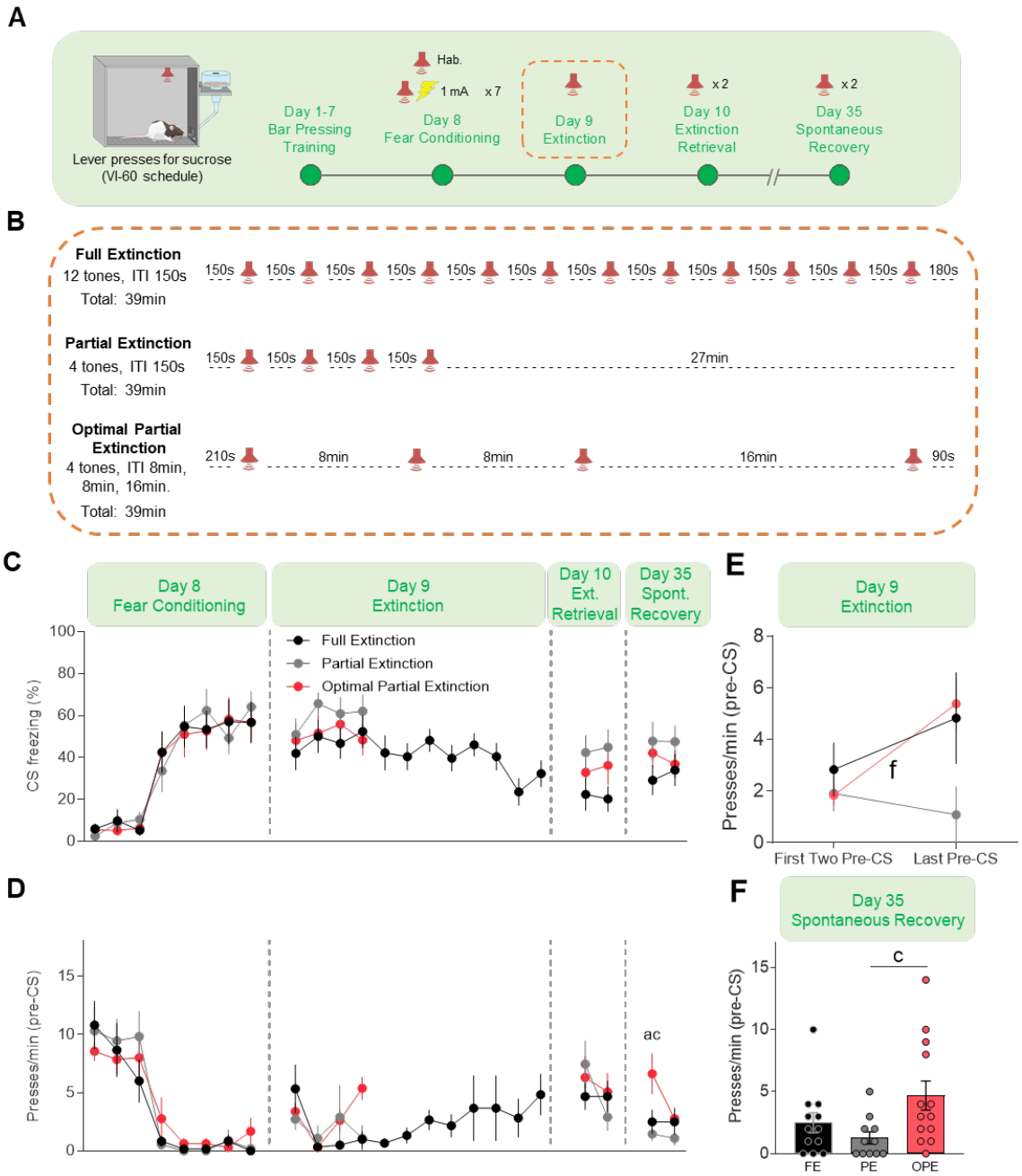

Figure 5. Computationally designed protocol enhanced fear extinction in rats. **A.** Schematic of the enhanced fear extinction experimental procedures. Rats were trained to constantly press a lever to retrieve sucrose pellets in a variable interval 60 (VI60) schedule, where the average interval between each sucrose delivery is 60 s. **B,** Schematics of the fear extinction protocols for full extinction (FE, n = 12), partial extinction (PE, n = 11), and optimal partial extinction groups (OPE, n = 13), during which rats

received multiple trials of a conditioned stimulus (CS, 3 kHz tone, 30 s). **C,** Freezing levels during CS presentations of each group across the experiment. No significant difference between groups was found by Two-way RM ANOVA. **D,** Lever presses rates during the 30s of each CS presentation (pre-CS period) of each group across the experiment. Two-way repeated-measure ANOVA for each day followed by Tukey's pairwise post hoc test. Letters a and c indicate pairwise tests with $p < 0.05$: a, FE vs. OPE ; c, OPE vs. PE. **E,** OPE group shows significant increase of pre-CS lever presses comparing the last CS presentation to the average lever press rate of the first two CS presentations. Paired Student's t test. Letter f indicates test with $p < 0.05$: OPC, Last 4 CS vs. First 4 CS. **F,** OPE group shows higher lever presses during pre-CS period compared to PE group in spontaneous recovery test. One-way ANOVA followed by Tukey's post hoc test. Letter c indicates pairwise comparison with * $p<0.05$: OPE vs. PE.

DISCUSSION

Studies on nonassociative learning in invertebrates have provided significant insights about the molecular mechanisms of learning and memory due to their simplicity and tractability (Byrne and Hawkins, 2015; Kandel, 2001; Carew and Sahley, 1986). Long-term nonassociative learning in different regions of the nervous system or across different species shares many intracellular molecular cascades including cAMP-PKA and Raf-MEK-ERK signaling (Bartsch et al., 1995; Martin et al., 1997). These two pathways are also required for associative learning in invertebrates and mammals (Hawkins and Byrne, 2015; Schafe and LeDoux, 2000; Adams and Sweatt, 2002). The conservation of these mechanisms makes these molecular cascades potential candidates for a universal intervention to enhance learning and memory. We have previously demonstrated that a computationally designed protocol that maximizes the interaction between PKA and ERK pathways enhances LTF and nonassociative

611 learning in *Aplysia* (Zhang et al., 2011). Here, we extended the feasibility of this
612 computational approach to associative learning in mammals by adapting the simplified
613 mathematical model used in *Aplysia* to simulate the dynamics of PKA and ERK in rat
614 hippocampus based on empirical data available in the literature (Wang et al., 2014;
615 Roberson and Sweatt, 1996; Vázquez et al., 2000). After simulating ~1000 different
616 training protocols of auditory fear conditioning, we identified an optimal protocol with
617 irregular ITIs which resulted in stronger fear acquisition and extinction-resistant memory
618 formation in rats, when compared to either massed or spaced training protocols with
619 equal ITIs. Using a separate fear extinction paradigm, we also showed that an optimal
620 training protocol was sufficient to induce enhanced extinction of contextual fear memory
621 in rats, when compared to standard or partial extinction protocols with equal ITIs. Our
622 results demonstrate the power of a simplified model of intracellular signaling cascades
623 in guiding associative learning across species, attesting the essential role of the
624 interaction between PKA and ERK pathways in both nonassociative and associative
625 learning. In addition, our findings highlight the potential clinical relevance of using
626 computational modeling to enhance associative learning in patients with memory
627 deficits, as well as to enhance extinction-based exposure therapies in patients with
628 anxiety disorders.
629
630 Pioneering studies have demonstrated that training protocols using spaced ITIs result in
631 stronger memory acquisition than those using standard massed ITIs, a well-established
632 phenomenon described as the “trial-spacing effect” (see review by Smolen et al., 2016).
633 Data demonstrating this effect in animals and humans illustrate the relationship between

634 the duration of the ITIs and the strength of memory formation as an inverted-U-shape
635 curve (Verkoeijen et al., 2005; Barela, 1999), consistent with our simulated results (Fig.
636 1C). Previous findings have attributed this spacing effect to the different efficacy of
637 massed vs. spaced protocols in inducing LTP/LTF through plasticity-related signaling.
638 For instance, spaced training protocols in rodents lead to increased activation of ERK
639 (Ajay and Bhalla, 2007), followed by CREB phosphorylation and the expression of
640 downstream genes, which have not been reported following massed training protocols
641 in the same species (Genoux et al., 2002). A computational model based on slice
642 electrophysiology from rat hippocampal data has found that the peak of ERK activation
643 aligns with the optimal ITI for LTP induction (Ajay and Bhalla, 2004). Although that study
644 provided a possible mechanism for the trial-spacing effect and a potential approach to
645 identify more effective protocols for associative learning, it relied on fixed ITIs that are
646 not necessarily the optimal intervals to induce synaptic plasticity and LTM. In fact, our
647 simulations showed that an optimal protocol with irregular ITIs was superior to most
648 spaced protocols with the same number of trials and equal ITIs. In the fear conditioning
649 experiment, the optimal protocol induced stronger and persistent fear memory in rats,
650 when compared to a spaced protocol predicted to be the most efficient among protocols
651 with equal ITIs. These results suggest that the trial-spacing effect in mammals can be at
652 least partially explained by enhanced overlap between PKA and ERK pathways, which
653 are critical for CREB activation (Impey et al., 1998). More importantly, our findings
654 demonstrate that protocols that include irregular ITIs can be a better approach to
655 enhance learning than previous protocols using equal ITIs.
656

657 The enhanced performance of our optimal protocol (OPC) compared to a spaced
658 protocol (SPC) during fear conditioning appears constrained by the intensity of stimuli.
659 The model predicts higher performance for OPC when weak stimuli are used, but
660 comparable performance when strong stimuli are used (**Fig. 3A**). Drawing a line to
661 distinguish weak and strong footshock intensities is not straightforward because the
662 relationship between fear memory and footshock intensity is neither monotonic nor
663 linear (Davis and Astrachan, 1978). Nevertheless, we observed clear differences in the
664 efficacy of the optimal fear conditioning protocol when using footshocks of different
665 intensities. When we compared the optimal partial conditioning protocol to a massed
666 partial conditioning protocol using a standard footshock intensity (0.7 mA, **Fig.2**)
667 commonly used in previous studies (Abel et al., 1997), we found only small differences
668 in the conditioned responses (CS freezing) between the two protocols. However, when
669 we used a lower footshock intensity (0.5 mA, **Fig.3**) to compare the optimal partial
670 conditioning protocol to a spaced partial conditioning protocol, we found a significant
671 increase in CS freezing in the OPC group during fear acquisition, retrieval, and
672 spontaneous recovery tests. Considering the robustness of the trial-spacing effect, it is
673 possible that differences between the OPC and the massed PC groups at the higher
674 footshock intensity were masked by a “ceiling effect”. These data suggest that our
675 approach could be more beneficial for learning protocols relying on relatively weak
676 stimuli. Additional studies need to be conducted to understand the mechanism by which
677 the intensity of stimuli determines the enhanced performance of protocols with irregular
678 ITIs compared to protocols with fixed ITIs.
679

The association between the CS and US is primarily mediated by the lateral amygdala where LTP induces enhanced CS responses (see review by Maren, 2005; Johansen et al., 2011). Nevertheless, another important and distinguishable component of fear memory formation is the context in which the association has occurred. In the fear conditioning experiment, enhanced CS freezing by our computationally designed protocol was only observed in the same context where fear conditioning took place, suggesting that the memory facilitation effect induced by our optimal protocol is context dependent. Similarly, in the fear extinction experiment, enhancement by the optimal protocol was only observed during the pre-CS lever pressing, a more sensitive index of contextual fear memory during extinction and spontaneous recovery (Morgan and LeDoux, 1995; Padilla-Coreano et al., 2012; Woods and Bouton, 2008; Mast et al., 1982; Sotres-Bayon et al., 2012). These results are consistent with the fact that the model is based on empirical data from rat hippocampus currently available in the literature. The hippocampus plays major roles in context encoding during fear conditioning, fear extinction, and the time-dependent reappearance of fear following extinction training (*i.e.*, spontaneous recovery) (see reviews by Maren et al., 2013; Bouton et al., 2021). The observation that the temporal dynamics of ERK pathways differ across brain regions involved in fear memory, with peaks occurring at 20 min after stimulation in the hippocampus versus 60 min after fear conditioning in the lateral amygdala (Schafe et al., 2000; Di Benedetto et al., 2009; Wang et al., 2014) , suggests that the model may be able to predict optimal protocols targeting specific components of fear memory based on the dynamics of intracellular signaling cascades in distinct brain regions. Future studies will test this possibility by modeling the molecular cascades in

703 the lateral amygdala to preferentially target the acquisition and extinction of CS-
704 associated memories.
705
706 It is worth noting that the model is an extremely simplified one. We did not consider
707 many other important molecular cascades important for LTP and memory formation. For
708 example, calcium/calmodulin-dependent protein kinase II (CaMKII) and protein kinase C
709 (PKC) are also required for LTP induction (Smolen et al., 2020; Malenka et al., 1989;
710 Wang et al., 2016). In addition, we built the model with empirical data of PKA and ERK
711 dynamics from the literature, which are based on *ex vivo* analyses and have limited
712 temporal resolution. However, despite these limitations, we demonstrated that the
713 simplified model using essential biochemical cascades for learning and memory was
714 sufficient to enhance associative learning in three different experiments in mammals. A
715 more complex model that incorporates a wider range of intracellular and extracellular
716 processes based on *in vivo* real-time data may strengthen the predictive ability of
717 simulations. Further experiments should also investigate whether the memory
718 enhancing effects of our optimal protocol vary across subjects of different sexes and
719 ages, as well as its efficacy in animal models of cognitive impairment. Together, our
720 results suggest the possibility of using similar model-driven, non-invasive behavioral
721 approaches in preclinical and clinical studies aimed at enhancing learning or restoring
722 memory deficits in humans.
723
724
725

AUTHOR CONTRIBUTIONS

X.O.Z, D.S.E., and C.E.C performed and analyzed the behavioral experiments. Y.Z. implemented the computational model and ran all simulations. P.S. helped design and implement the computational model. F.H.D-M and J.H.B supervised and contributed to all aspects of this study. All the authors participated in the design of the experiments. X.O.Z. and F.H.D-M interpreted the data and prepared the manuscript with comments from all the co-authors.

ACKNOWLEDGEMENT

We thank Nikita Watson and Sharon Gordon for their technical and administrative assistance. We also thank current members of the Byrne and Do Monte and Labs for their valuable comments on the manuscript. This work was supported by NIH grant R01-NS102490 to J.H.B, and NIH grant R00-MH105549, NIH grant R01-MH120136, a Brain & Behavior Research Foundation grant (NARSAD Young Investigator), and a Rising STARs Award from UT System to F.H.D-M.

COMPETING INTERESTS

The authors declare no competing interests.

746 **REFERENCES**

747 Abel T, Nguyen PV, Barad M, Deuel TA, Kandel ER, Bourtchouladze R (1997) Genetic
748 demonstration of a role for pka in the late phase of ltp and in hippocampus-based
749 long-term memory. Cell 88:615-626.

750 Adams JP, Sweatt JD (2002) Molecular psychology: Roles for the erk map kinase
751 cascade in memory. Annu Rev Pharmacol Toxicol 42:135-163.

752 Ajay SM, Bhalla US (2004) A role for erkii in synaptic pattern selectivity on the time-
753 scale of minutes. Eur J Neurosci 20:2671-2680.

754 Ajay SM, Bhalla US (2007) A propagating erkii switch forms zones of elevated dendritic
755 activation correlated with plasticity. HFSP J 1:49-66.

756 Alberini CM (2009) Transcription factors in long-term memory and synaptic plasticity.
757 Physiol Rev 89:121-145.

758 Anderson MJ, Jablonski SA, Klimas DB (2008) Spaced initial stimulus familiarization
759 enhances novelty preference in long-evans rats. Behav Processes 78:481-486.

760 Barela PB (1999) Theoretical mechanisms underlying the trial-spacing effect in
761 pavlovian fear conditioning. Journal of Experimental Psychology: Animal
762 Behavior Processes 25:177.

763 Bartsch D, Ghirardi M, Skehel PA, Karl KA, Herder SP, Chen M, Bailey CH, Kandel ER
764 (1995) Aplysia creb2 represses long-term facilitation: Relief of repression
765 converts transient facilitation into long-term functional and structural change. Cell
766 83:979-992.

767 Berman DE, Dudai Y (2001) Memory extinction, learning anew, and learning the new:
768 Dissociations in the molecular machinery of learning in cortex. Science
769 291:2417-2419.
770 Bouton ME, Maren S, McNally GP (2021) Behavioral and neurobiological mechanisms
771 of pavlovian and instrumental extinction learning. Physiol Rev 101:611-681.
772 Brown MT, Tan KR, O'Connor EC, Nikonenko I, Muller D, Luscher C (2012) Ventral
773 tegmental area gaba projections pause accumbal cholinergic interneurons to
774 enhance associative learning. Nature 492:452-456.
775 Byrne JH, Hawkins RD (2015) Nonassociative learning in invertebrates. Cold Spring
776 Harb Perspect Biol 7.
777 Cain CK, Blouin AM, Barad M (2003) Temporally massed cs presentations generate
778 more fear extinction than spaced presentations. J Exp Psychol Anim Behav
779 Process 29:323-333.
780 Carew TJ, Sahley CL (1986) Invertebrate learning and memory: From behavior to
781 molecules. Annu Rev Neurosci 9:435-487.
782 Cepeda NJ, Pashler H, Vul E, Wixted JT, Rohrer D (2006) Distributed practice in verbal
783 recall tasks: A review and quantitative synthesis. Psychol Bull 132:354-380.
784 Dash PK, Hochner B, Kandel ER (1990) Injection of the camp-responsive element into
785 the nucleus of aplysia sensory neurons blocks long-term facilitation. Nature
786 345:718-721.
787 Davis M, Astrachan DI (1978) Conditioned fear and startle magnitude: Effects of
788 different footshock or backshock intensities used in training. J Exp Psychol Anim
789 Behav Process 4:95-103.

790 de Oliveira Alvares L, Do-Monte FH (2021) Understanding the dynamic and destiny of
791 memories. Neurosci Biobehav Rev 125:592-607.
792 Detert JA, Kampa ND, Moyer JR, Jr. (2008) Differential effects of training intertrial
793 interval on acquisition of trace and long-delay fear conditioning in rats. Behav
794 Neurosci 122:1318-1327.
795 Di Benedetto B, Kallnik M, Weisenhorn DM, Falls WA, Wurst W, Holter SM (2009)
796 Activation of erk/mapk in the lateral amygdala of the mouse is required for
797 acquisition of a fear-potentiated startle response. Neuropsychopharmacology
798 34:356-366.
799 Do-Monte FH, Manzano-Nieves G, Quinones-Laracuente K, Ramos-Medina L, Quirk GJ
800 (2015) Revisiting the role of infralimbic cortex in fear extinction with optogenetics.
801 J Neurosci 35:3607-3615.
802 Ermentrout B (2002) Simulating, analyzing, and animating dynamical systems : A guide
803 to xppaut for researchers and students. Philadelphia: Society for Industrial and
804 Applied Mathematics.
805 Fernandez SM, Lewis MC, Pechenino AS, Harburger LL, Orr PT, Gresack JE, Schafe
806 GE, Frick KM (2008) Estradiol-induced enhancement of object memory
807 consolidation involves hippocampal extracellular signal-regulated kinase
808 activation and membrane-bound estrogen receptors. J Neurosci 28:8660-8667.
809 Flood JF, Jarvik ME, Bennett EL, Orme AE, Rosenzweig MR (1977) Protein synthesis
810 inhibition and memory for pole jump active avoidance and extinction. Pharmacol
811 Biochem Behav 7:71-77.

812 Genoux D, Haditsch U, Knobloch M, Michalon A, Storm D, Mansuy IM (2002) Protein
813 phosphatase 1 is a molecular constraint on learning and memory. Nature
814 418:970-975.
815 Goldsmith BA, Abrams TW (1991) Reversal of synaptic depression by serotonin at
816 aplysia sensory neuron synapses involves activation of adenylyl cyclase. Proc
817 Natl Acad Sci U S A 88:9021-9025.
818 Goode TD, Maren S (2014) Animal models of fear relapse. ILAR J 55:246-258.
819 Hawkins RD, Byrne JH (2015) Associative learning in invertebrates. Cold Spring Harb
820 Perspect Biol 7.
821 Holmes A, Quirk GJ (2010) Pharmacological facilitation of fear extinction and the search
822 for adjunct treatments for anxiety disorders--the case of yohimbine. Trends
823 Pharmacol Sci 31:2-7.
824 Impey S, Obrietan K, Wong ST, Poser S, Yano S, Wayman G, Deloulme JC, Chan G,
825 Storm DR (1998) Cross talk between erk and pka is required for ca2+ stimulation
826 of creb-dependent transcription and erk nuclear translocation. Neuron 21:869-
827 883.
828 Jiang L, Wang L, Yin Y, Huo M, Liu C, Zhou Q, Yu D, Xu L, Mao R (2019) Spaced
829 training enhances contextual fear memory via activating hippocampal 5-ht2a
830 receptors. Front Mol Neurosci 12:317.
831 Johansen JP, Cain CK, Ostroff LE, LeDoux JE (2011) Molecular mechanisms of fear
832 learning and memory. Cell 147:509-524.
833 Kandel ER (2001) The molecular biology of memory storage: A dialogue between genes
834 and synapses. Science 294:1030-1038.

835 Lauterborn JC, Palmer LC, Jia Y, Pham DT, Hou B, Wang W, Trieu BH, Cox CD,
836 Kantorovich S, Gall CM, Lynch G (2016) Chronic ampakine treatments stimulate
837 dendritic growth and promote learning in middle-aged rats. J Neurosci 36:1636-
838 1646.
839 Lee K, Holley SM, Shobe JL, Chong NC, Cepeda C, Levine MS, Masmanidis SC (2017)
840 Parvalbumin interneurons modulate striatal output and enhance performance
841 during associative learning. Neuron 93:1451-1463 e1454.
842 Liu RY, Cleary LJ, Byrne JH (2011) The requirement for enhanced creb1 expression in
843 consolidation of long-term synaptic facilitation and long-term excitability in
844 sensory neurons of aplysia. J Neurosci 31:6871-6879.
845 Liu X, Ramirez S, Pang PT, Puryear CB, Govindarajan A, Deisseroth K, Tonegawa S
846 (2012) Optogenetic stimulation of a hippocampal engram activates fear memory
847 recall. Nature 484:381-385.
848 Lonsdorf TB et al. (2017) Don't fear 'fear conditioning': Methodological considerations
849 for the design and analysis of studies on human fear acquisition, extinction, and
850 return of fear. Neurosci Biobehav Rev 77:247-285.
851 Lynch G, Cox CD, Gall CM (2014) Pharmacological enhancement of memory or
852 cognition in normal subjects. Front Syst Neurosci 8:90.
853 Lynch MA (2004) Long-term potentiation and memory. Physiol Rev 84:87-136.
854 Malenka RC, Kauer JA, Perkel DJ, Mauk MD, Kelly PT, Nicoll RA, Waxham MN (1989)
855 An essential role for postsynaptic calmodulin and protein kinase activity in long-
856 term potentiation. Nature 340:554-557.

857 Maren S (2005) Synaptic mechanisms of associative memory in the amygdala. Neuron
858 47:783-786.
859 Maren S, Phan KL, Liberzon I (2013) The contextual brain: Implications for fear
860 conditioning, extinction and psychopathology. Nat Rev Neurosci 14:417-428.
861 Martin KC, Michael D, Rose JC, Barad M, Casadio A, Zhu H, Kandel ER (1997) Map
862 kinase translocates into the nucleus of the presynaptic cell and is required for
863 long-term facilitation in aplysia. Neuron 18:899-912.
864 Martin SJ, Grimwood PD, Morris RG (2000) Synaptic plasticity and memory: An
865 evaluation of the hypothesis. Annu Rev Neurosci 23:649-711.
866 Mast M, Blanchard RJ, Blanchard DC (1982) The relationship of freezing and response
867 suppression in a cer situation. In, pp 151-167. US: Kenyon Coll Psychology Dept.
868 Mayes A, Montaldi D, Migo E (2007) Associative memory and the medial temporal
869 lobes. Trends Cogn Sci 11:126-135.
870 McDougal RA, Morse TM, Hines ML, Shepherd GM (2015) Modelview for modeldb:
871 Online presentation of model structure. Neuroinformatics 13:459-470.
872 McGaugh JL, Petrinovich LF (1965) Effects of drugs on learning and memory. Int Rev
873 Neurobiol 8:139-196.
874 Milner B, Squire LR, Kandel ER (1998) Cognitive neuroscience and the study of
875 memory. Neuron 20:445-468.
876 Morgan MA, LeDoux JE (1995) Differential contribution of dorsal and ventral medial
877 prefrontal cortex to the acquisition and extinction of conditioned fear in rats.
878 Behav Neurosci 109:681-688.

879 Muller U, Carew TJ (1998) Serotonin induces temporally and mechanistically distinct
880 phases of persistent pka activity in aplysia sensory neurons. Neuron 21:1423-
881 1434.
882 Nabavi S, Fox R, Proulx CD, Lin JY, Tsien RY, Malinow R (2014) Engineering a
883 memory with ltd and ltp. Nature 511:348-352.
884 Nakazawa K, Quirk MC, Chitwood RA, Watanabe M, Yeckel MF, Sun LD, Kato A, Carr
885 CA, Johnston D, Wilson MA, Tonegawa S (2002) Requirement for hippocampal
886 ca3 nmda receptors in associative memory recall. Science 297:211-218.
887 Padilla-Coreano N, Do-Monte FH, Quirk GJ (2012) A time-dependent role of midline
888 thalamic nuclei in the retrieval of fear memory. Neuropharmacology 62:457-463.
889 Philips GT, Tzvetkova EI, Carew TJ (2007) Transient mitogen-activated protein kinase
890 activation is confined to a narrow temporal window required for the induction of
891 two-trial long-term memory in aplysia. J Neurosci 27:13701-13705.
892 Phillips RG, LeDoux JE (1992) Differential contribution of amygdala and hippocampus
893 to cued and contextual fear conditioning. Behav Neurosci 106:274-285.
894 Podlesnik CA, Kelley ME, Jimenez-Gomez C, Bouton ME (2017) Renewed behavior
895 produced by context change and its implications for treatment maintenance: A
896 review. J Appl Behav Anal 50:675-697.
897 Quirk GJ, Mueller D (2008) Neural mechanisms of extinction learning and retrieval.
898 Neuropsychopharmacology 33:56-72.
899 Quirk GJ, Russo GK, Barron JL, Lebron K (2000) The role of ventromedial prefrontal
900 cortex in the recovery of extinguished fear. J Neurosci 20:6225-6231.

901 Radulovic J, Tronson NC (2010) Molecular specificity of multiple hippocampal
902 processes governing fear extinction. Rev Neurosci 21:1-17.
903 Raman M, McLaughlin K, Violato C, Rostom A, Allard JP, Coderre S (2010) Teaching in
904 small portions dispersed over time enhances long-term knowledge retention.
905 Med Teach 32:250-255.
906 Roberson ED, Sweatt JD (1996) Transient activation of cyclic amp-dependent protein
907 kinase during hippocampal long-term potentiation. The Journal of biological
908 chemistry 271:30436-30441.
909 Santini E, Muller RU, Quirk GJ (2001) Consolidation of extinction learning involves
910 transfer from nmda-independent to nmda-dependent memory. J Neurosci
911 21:9009-9017.
912 Santini E, Ge H, Ren K, Pena de Ortiz S, Quirk GJ (2004) Consolidation of fear
913 extinction requires protein synthesis in the medial prefrontal cortex. J Neurosci
914 24:5704-5710.
915 Schacher S, Castellucci VF, Kandel ER (1988) Camp evokes long-term facilitation in
916 aplysia sensory neurons that requires new protein synthesis. Science 240:1667-
917 1669.
918 Schafe GE, LeDoux JE (2000) Memory consolidation of auditory pavlovian fear
919 conditioning requires protein synthesis and protein kinase a in the amygdala. J
920 Neurosci 20:RC96.
921 Schafe GE, Atkins CM, Swank MW, Bauer EP, Sweatt JD, LeDoux JE (2000) Activation
922 of erk/map kinase in the amygdala is required for memory consolidation of
923 pavlovian fear conditioning. J Neurosci 20:8177-8187.

924 Scharf MT, Woo NH, Lattal KM, Young JZ, Nguyen PV, Abel T (2002) Protein synthesis
925 is required for the enhancement of long-term potentiation and long-term memory
926 by spaced training. J Neurophysiol 87:2770-2777.
927 Selden NR, Everitt BJ, Jarrard LE, Robbins TW (1991) Complementary roles for the
928 amygdala and hippocampus in aversive conditioning to explicit and contextual
929 cues. Neuroscience 42:335-350.
930 Sharif S, Guirguis A, Fergus S, Schifano F (2021) The use and impact of cognitive
931 enhancers among university students: A systematic review. Brain Sci 11.
932 Sharma SK, Carew TJ (2004) The roles of mapk cascades in synaptic plasticity and
933 memory in aplysia: Facilitatory effects and inhibitory constraints. Learn Mem
934 11:373-378.
935 Sharma SK, Sherff CM, Shobe J, Bagnall MW, Sutton MA, Carew TJ (2003) Differential
936 role of mitogen-activated protein kinase in three distinct phases of memory for
937 sensitization in aplysia. J Neurosci 23:3899-3907.
938 Smolen P, Zhang Y, Byrne JH (2016) The right time to learn: Mechanisms and
939 optimization of spaced learning. Nat Rev Neurosci 17:77-88.
940 Smolen P, Baxter DA, Byrne JH (2020) Comparing theories for the maintenance of late
941 ltp and long-term memory: Computational analysis of the roles of kinase
942 feedback pathways and synaptic reactivation. Front Comput Neurosci
943 14:569349.
944 Sotres-Bayon F, Sierra-Mercado D, Pardilla-Delgado E, Quirk GJ (2012) Gating of fear
945 in prelimbic cortex by hippocampal and amygdala inputs. Neuron 76:804-812.

946 Szapiro G, Vianna MR, McGaugh JL, Medina JH, Izquierdo I (2003) The role of nmda
947 glutamate receptors, pka, mapk, and camkii in the hippocampus in extinction of
948 conditioned fear. Hippocampus 13:53-58.
949 Tronson NC, Schrick C, Fischer A, Sananbenesi F, Pages G, Pouyssegur J, Radulovic
950 J (2008) Regulatory mechanisms of fear extinction and depression-like behavior.
951 Neuropsychopharmacology 33:1570-1583.
952 Vázquez SI, Vázquez A, Peña de Ortiz S (2000) Different hippocampal activity profiles
953 for pka and pkc in spatial discrimination learning. Behavioral Neuroscience
954 114:1109-1118.
955 Verkoeijen PP, Rikers RM, Schmidt HG (2005) Limitations to the spacing effect:
956 Demonstration of an inverted u-shaped relationship between interrepetition
957 spacing and free recall. Exp Psychol 52:257-263.
958 Wang S, Sheng T, Ren S, Tian T, Lu W (2016) Distinct roles of pkciota/lambda and
959 pkmzeta in the initiation and maintenance of hippocampal long-term potentiation
960 and memory. Cell Rep 16:1954-1961.
961 Wang Y, Zhu G, Briz V, Hsu YT, Bi X, Baudry M (2014) A molecular brake controls the
962 magnitude of long-term potentiation. Nature communications 5:3051.
963 Woods AM, Bouton ME (2008) Immediate extinction causes a less durable loss of
964 performance than delayed extinction following either fear or appetitive
965 conditioning. Learn Mem 15:909-920.
966 Zhang Y, Smolen PD, Cleary LJ, Byrne JH (2021) Quantitative description of the
967 interactions among kinase cascades underlying long-term plasticity of aplysia
968 sensory neurons. Scientific reports 11:14931.

969 Zhang Y, Liu RY, Heberton GA, Smolen P, Baxter DA, Cleary LJ, Byrne JH (2011)
970 Computational design of enhanced learning protocols. Nat Neurosci 15:294-297.
971
972
973
974
975
976
977
978
979
980
981
982
983
984
985
986
987
988
989
990
991

SUPPLEMENTARY FIGURES

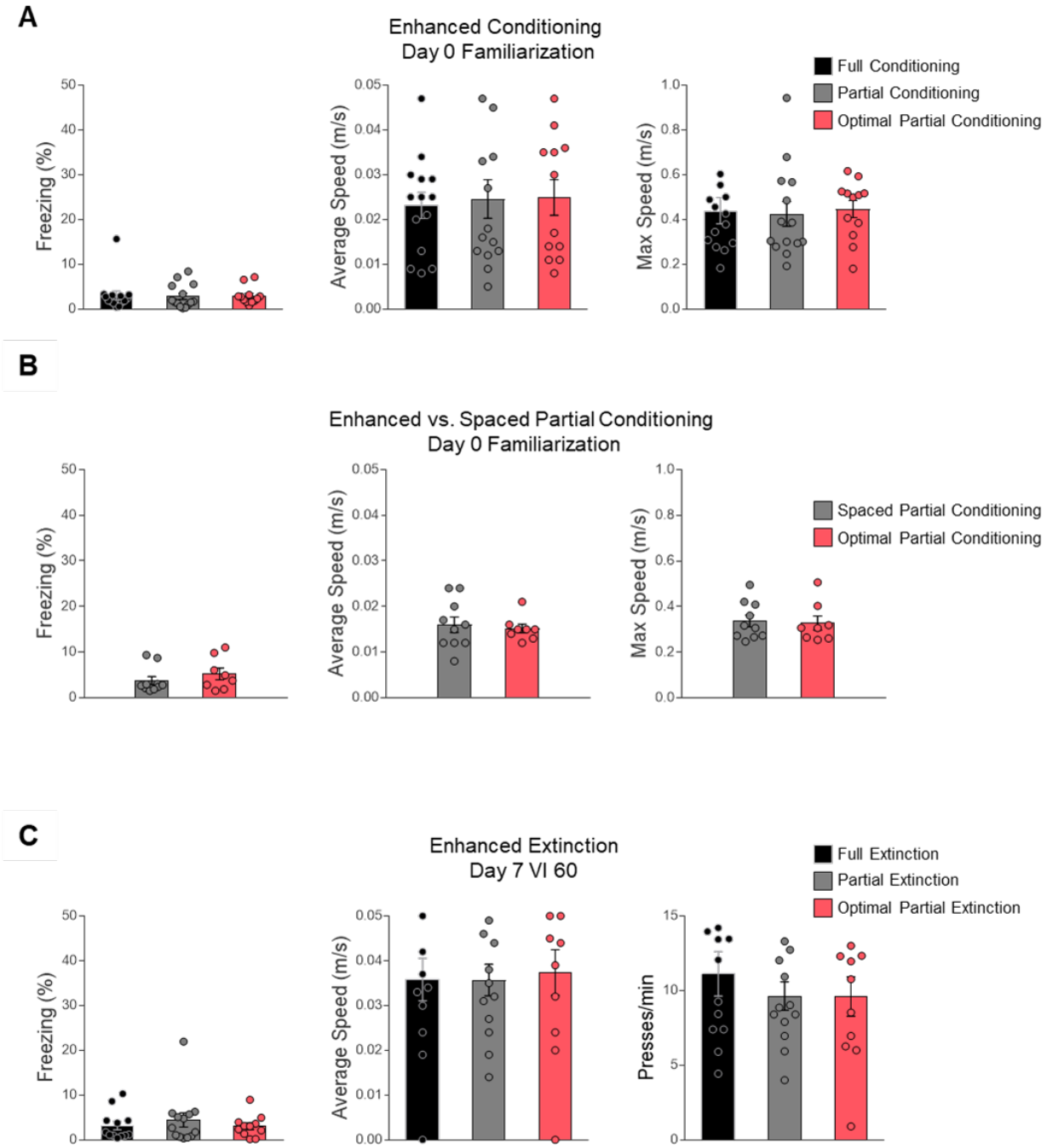

Supplementary Figure 1. No difference of baseline activity between groups. A, No differences in total freezing level (left), average speed (middle), and maximum speed (right) between the three groups were observed during familiarization of the enhanced conditioning experiment. **B,** No differences in total freezing level (left), average speed (middle), and maximum speed (right) were seen between the three

groups during familiarization of the enhanced vs. spaced conditioning experiment. **C,** No differences in total freezing level (left), average speed (middle), and rate of lever presses (right) were observed between the three groups during the last day of lever presses training of the enhanced extinction experiment. One-way ANOVA. Data shown as mean ± SEM.

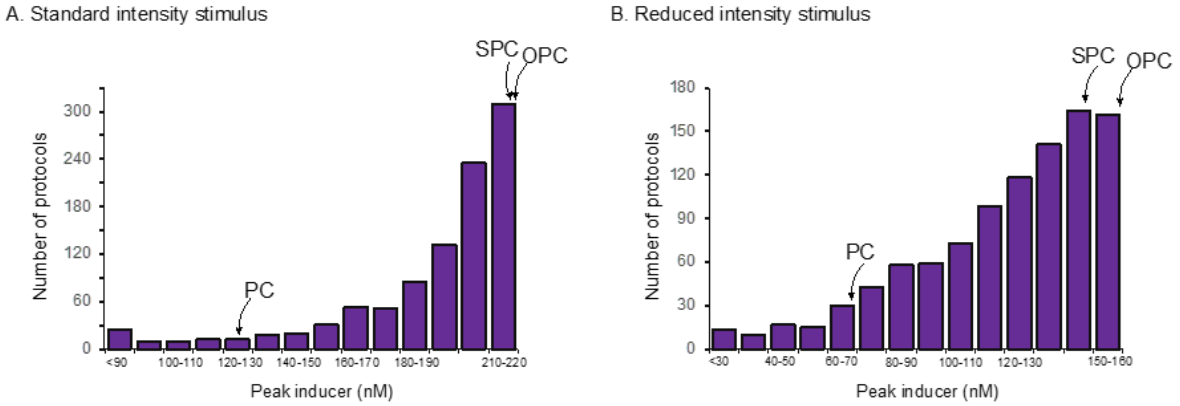

Supplementary Figure 2. **Histogram of peak levels of inducer from 1,000 protocols.** (A) Standard intensity stimulus (*Stim* = 300 μM). The range of peak levels of inducer (0 nM - 220 nM) was subdivided into 14 bins, and the number of simulations that produced a peak concentration of inducer in each subdivision was plotted. The arrows indicate which bins contained the peak concentrations produced by the partial conditioning, spaced partial conditioning (SPC), and the optimal partial conditioning (OPC) protocols. (B) Reduced intensity stimulus (*Stim* = 200 μM). The range of peak levels of inducer (0 nM - 160 nM) was subdivided into 14 bins, and the number of simulations that produced a peak concentration of inducer in each subdivision was plotted.

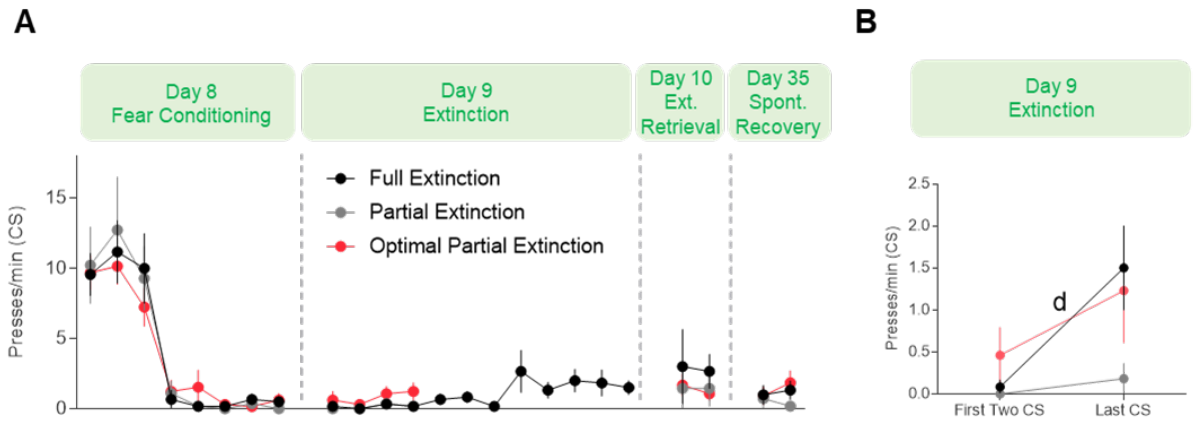

Supplementary Figure 3. Lever press during CS presentations in enhanced extinction experiment. **A**, Lever presses rates during CS presentations of each group across the experiment. Two-way repeated-measure ANOVA for each day found no difference among groups. **B,** FE group shows significant increase of CS lever presses comparing the last CS presentation to the average lever press rate of the first two CS presentations. Paired Student's t test. Letter d indicate test with $p < 0.05$: d, FE: Last 4 CS vs. First 4 CS.